REPORT DOCUMENTATION PAGE

Form Approved
OMB No. 0704-0188

1. REPORT DATE *(DD-MM-YYYY)* July 2015	**2. REPORT TYPE** Technical Paper	**3. DATES COVERED** *(From - To)* July 2015-July 2015
4. TITLE AND SUBTITLE Time-Synchronized Continuous Wave Laser Induced Fluorescence Velocity Measurements of a 600 Watt Hall Thruster		**5a. CONTRACT NUMBER** In-House
		5b. GRANT NUMBER
		5c. PROGRAM ELEMENT NUMBER
6. AUTHOR(S) Natalia MacDonald-Tenenbaum, Christopher Young, Andrea Lucca Fabris, Michael Nakles, Mark Cappelli, and William Hargus Jr.		**5d. PROJECT NUMBER**
		5e. TASK NUMBER
		5f. WORK UNIT NUMBER Q1AU
7. PERFORMING ORGANIZATION NAME(S) AND ADDRESS(ES) Air Force Research Laboratory (AFMC) AFRL/RQRS 1 Ara Drive. Edwards AFB, CA 93524-7013		**8. PERFORMING ORGANIZATION REPORT NO.**
9. SPONSORING / MONITORING AGENCY NAME(S) AND ADDRESS(ES) Air Force Research Laboratory (AFMC) AFRL/RQR 5 Pollux Drive Edwards AFB CA 93524-7048		**10. SPONSOR/MONITOR'S ACRONYM(S)**
		11. SPONSOR/MONITOR'S REPORT NUMBER(S) **AFRL-RQ-ED-TP-2015-198**

12. DISTRIBUTION / AVAILABILITY STATEMENT
Distribution A: Approved for Public Release; Distribution Unlimited.

13. SUPPLEMENTARY NOTES
Technical Paper and Briefing Charts presented at The 34th International Electric Propulsion Conference; Kobe, Japan; 6-10 July 2015. PA#15329

14. ABSTRACT
A time-synchronized continuous wave laser induced fluorescence diagnostic technique based on a sample hold scheme is applied to xenon ion velocimetry of a BHT-600 Hall thruster plume. This method is capable of correlating measured fluorescence excitation line shapes with current fluctuations in a plasma discharge and is tolerant of natural drifting in the current oscillation frequency. This paper presents time-synchronized axial ion velocity measurements in the channel and near-field plume region of a 600 W Hall thruster operating on xenon. Results show significant fluctuations in LIF signal intensity (correlated with the density of the probed excited metastable state) in time during the discharge current cycle, with the peak intensity occurring at the discharge current maximum. Measured ion velocities also fluctuate in time with the current oscillation, reaching their peak after the discharge current maximum. This work provides detailed insight into the complex, time-dependent ionization and ion acceleration mechanisms in the channel of a Hall thruster that would be unattainable with a time-averaged measurement.

15. SUBJECT TERMS

16. SECURITY CLASSIFICATION OF:			**17. LIMITATION OF ABSTRACT**	**18. NUMBER OF PAGES**	**19a. NAME OF RESPONSIBLE PERSON**
					William Hargus
a. REPORT	**b. ABSTRACT**	**c. THIS PAGE**	SAR	23	**19b. TELEPHONE NO** *(include area code)*
Unclassified	**Unclassified**	**Unclassified**			

Standard Form 298 (Rev. 8-98)
Prescribed by ANSI Std. 239.18

Time-Synchronized Continuous Wave Laser Induced Fluorescence Velocity Measurements of a 600 Watt Hall Thruster

IEPC-2015-350/ISTS-2015-b-350

Presented at Joint Conference of 30th International Symposium on Space Technology and Science, 34th International Electric Propulsion Conference and 6th Nano-satellite Symposium
Hyogo-Kobe, Japan
July 4–10, 2015

Natalia MacDonald-Tenenbaum*
Air Force Research Laboratory, Edwards AFB, CA, 93524, USA

Christopher V. Young† and Andrea Lucca Fabris‡
Stanford Plasma Physics Laboratory, Stanford, CA, 94305, USA

Michael Nakles§
ERC, Inc., Air Force Research Laboratory, Edwards AFB, CA, 93524, USA

William Hargus Jr.¶
Air Force Research Laboratory, Edwards AFB, CA, 93524, USA

and

Mark A. Cappelli‖
Stanford Plasma Physics Laboratory, Stanford, CA, 94305, USA

A time-synchronized continuous wave laser induced fluorescence diagnostic technique based on a sample hold scheme is applied to xenon ion velocimetry of a BHT-600 Hall thruster plume. This method is capable of correlating measured fluorescence excitation lineshapes with current fluctuations in a plasma discharge and is tolerant of natural drifting in the current oscillation frequency. This paper presents time-synchronized axial ion velocity measurements in the channel and near-field plume region of a 600 W Hall thruster operating on xenon. Results show significant fluctuations in LIF signal intensity (correlated with the density of the probed excited metastable state) in time during the discharge current cycle, with the peak intensity occurring at the discharge current maximum. Measured ion velocities also fluctuate in time with the current oscillation, reaching their peak after the discharge current maximum. This work provides detailed insight into the complex, time-dependent ionization and ion acceleration mechanisms in the channel of a Hall thruster that would be unattainable with a time-averaged measurement.

*Researcher, In-Space Propulsion Branch, natalia.macdonald@us.af.mil
†PhD Candidate, Mechanical Engineering Department, cvyoung@stanford.edu
‡Postdoctoral Research Fellow, Mechanical Engineering Department, lfandrea@stanford.edu
§Reseacher, In-Space Propulsion Branch, michael.nakles.ctr@us.af.mil
¶Program Manager, In-Space Propulsion Branch, william.hargus@us.af.mil
‖Professor, Mechanical Engineering Department, cap@stanford.edu

I. Introduction

MEASURING time resolved properties in oscillatory plasma discharges such as Hall thrusters is of great importance to understanding the physics behind their operation. Time varying properties such as the ion velocity distribution function (IVDF) can be directly linked to performance metrics, and are critical in validating numerical simulations that can be used to aid future development efforts. A powerful diagnostic for measuring ion velocities is laser induced fluorescence (LIF).[1]

LIF provides the opportunity to investigate plasma sources non-intrusively with higher spatial resolution (typically < 1 mm) than can be obtained with the more disruptive probes such as retarding potential analyzers. While the use of a pulsed laser system for time-resolved LIF velocimetry may seem attractive, the narrow spectral linewidth of the $5d[4]_{7/2} - 6p[3]_{5/2}$ xenon ion transition typically used for LIF velocimetry measurements of Hall thrusters[2,3] precludes the use of pulsed lasers with their characteristic linewidths being larger than that of the target transition. In order to accurately resolve this transition's spectral features and be able to derive accurate ion velocity distribution functions, narrow linewidth continuous-wave (CW) lasers are necessary for this application. CW lasers do not immediately lend themselves towards time resolved measurements, and thus several methods have been developed in recent years to achieve time resolution for LIF with a CW laser.

Pelissier et al. demonstrated a time-resolved photon-counting technique to detect LIF in the presence of a strong background emission.[4] This technique was further developed and applied to measuring IVDFs in Hall thrusters with externally stabilized oscillations by Mazouffre et al.[5,6] Durot et al. demonstrated a transfer function averaging technique applied to a hollow cathode discharge, forcing periodic current oscillations at 10 kHz.[7] Diallo et al. proposed a technique based on the Fourier decomposition of the periodic LIF signal and applied it to a Cylindrical Hall Thruster driven at 11.5 kHz.[8] Many of the preceding methods require a level of coherency in the periodic fluorescence signal attainable only through externally driving the current oscillation in question.

The sample-hold approach taken in this work relaxes the coherency requirement and synchronizes the fluorescence signal with the naturally drifting frequency of Hall thruster breathing mode oscillations. The breathing mode is the dominant low frequency (10-30 kHz) current oscillation observed in Hall thrusters that has been modeled as a propagating ionization front periodically traversing the channel.[9–11] Previous demonstrations of this method on a ~ 3 kHz current oscillation in a cusped field thruster[12] validated the technique, obtaining time-synchronized xenon ion velocity traces at a few spatial points. The technique was further demonstrated on a 350 W laboratory Hall thruster exhibiting ~ 20 kHz breathing mode oscillations.[13] Now, the hardware has been upgraded to permit measurement of a ~ 48 kHz Hall thruster breathing mode at a time resolution of 1 μs. Additionally, increased laser power has improved the measurement signal-to-noise characteristics. Data collection efficiency has been increased through parallelization, allowing simultaneous collection of LIF lineshapes synchronized with several temporal points (phases) along the current oscillation cycle.

The results presented below describe time-synchronized LIF velocimetry of a 600 W BHT-600 Hall thruster manufactured by Busek, Co. Axial xenon ion velocity distributions obtained with 1 μs time resolution are acquired at numerous locations throughout the discharge channel and into the near-field plume of the thruster. Temporally and spatially resolved changes in axial ion velocity throughout the discharge provide insight into the dynamics of propellant ionization and acceleration in these types of thrusters.

II. Experiment

A. BHT-600 Hall Thruster

Figure 1 shows a side view of the 600 W BHT-600 Hall thruster operating on xenon. The thruster acceleration channel has an outer radius of 32 mm, an inner radius of 24 mm, and 10 mm depth. The magnetic field is produced by four outer magnetic coils and one inner coil, which is operated independently to optimize the field topology. This thruster has been studied extensively using both electrostatic probes and various optical diagnostics.[14,15]

The operating conditions used in this work are outlined in Table 1. They are chosen to match the nominal operating point described in Gonzales et al.[16] to facilitate comparison. Typical discharge current and voltage characteristics of the BHT-600 are shown in Fig. 2, as well as the associated optical emission plus induced fluorescence signal recorded by a photomultiplier tube (PMT). FFTs of these traces show that the thruster

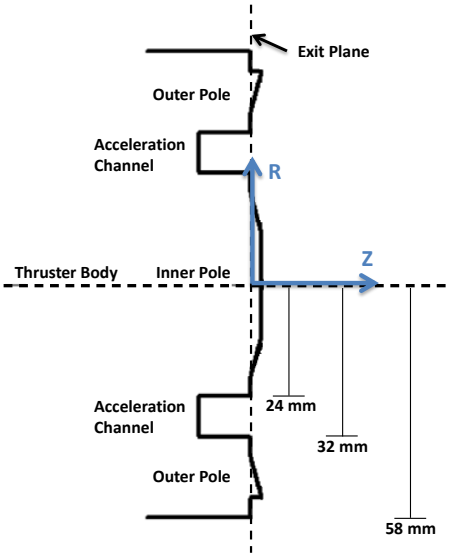

(a)

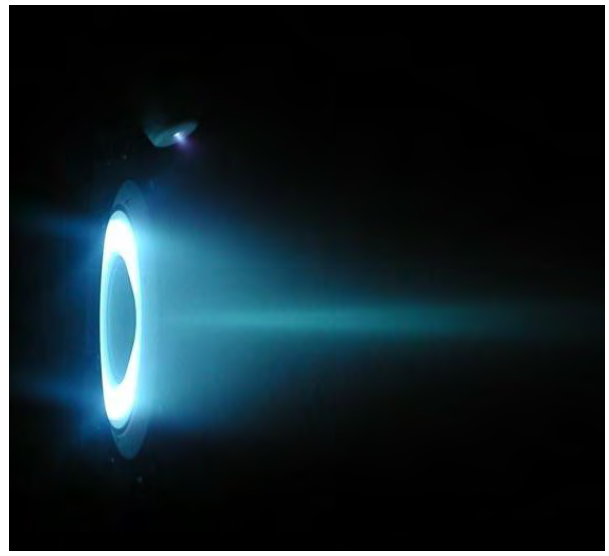

(b)

Figure 1: (a) Diagram of BHT-600 Hall thruster, including thruster dimensions and the coordinate system used in this work. (b) Side view of BHT-600 Hall thruster operating on xenon. The external cathode is visible above the thruster.

Table 1: BHT-600 Hall thruster nominal operating conditions.

Anode Flow	2.45 mg/s Xe (20.5 sccm)
Cathode Flow	197 μg/s Xe (1.5 sccm)
Anode Potential	300 V
Anode Current	2.05 A
Magnet 1 Current	2.0 A
Magnet 2 Current	2.0 A

oscillates quasi-periodically at a frequency of 48.4 ± 1.7 kHz, resulting in a typical current cycle with a period of 20.7 ± 0.7 μs.

B. Experimental Apparatus

LIF measurements for this study are performed in Chamber 6 at the Air Force Research Laboratory (AFRL) at Edwards AFB, CA. This facility is capable of achieving a background pressure of approximately 1.2×10^{-5} Torr (corrected for xenon) during thruster operation. The main optical train of this experimental apparatus has been described extensively elsewhere.[17] However, several upgrades have been made to this system to allow for more efficient data collection. These changes are depicted in Fig. 3.

Ion velocity measurements are accomplished by probing the $5d[4]_{7/2} - 6p[3]_{5/2}$ electronic transition of Xe II at 834.72 nm (air). The upper state of this transition is shared by the $6s[2]_{3/2} - 6p[3]_{5/2}$ transition at 541.92 nm,[18] used for non-resonant fluorescence collection. This transition has been utilized extensively throughout the electric propulsion community for time-averaged and time-resolved LIF velocimetry.[2,3,19,20] A New Focus Vortex TLB-6917 tunable diode laser is used to seed a TA-7600 VAMP tapered amplifier to achieve a probe beam output power of 60 mW. This is effectively 6× the power used in previous work,[21] but well within the linear regime of operation.

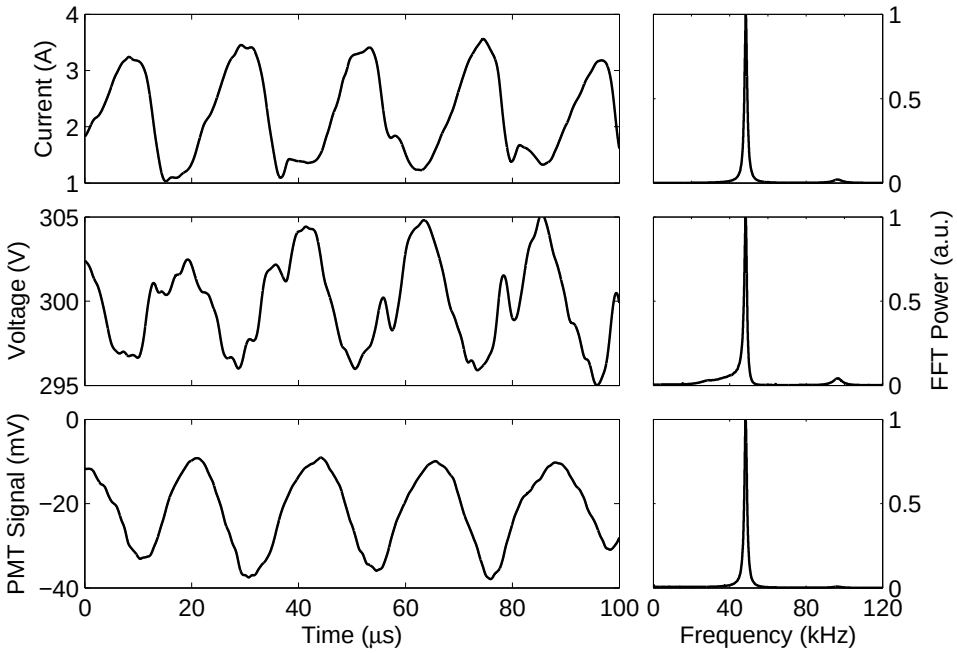

Figure 2: Current, Voltage, and photomultiplier (emission plus fluorescence) signals and their FFT's.

Beam pick-offs send portions of the beam into a Fabry-Perot (F-P) etalon for frequency reference, and an optogalvanic xenon reference cell (OGC) for a zero velocity spectral line reference. The additional laser power allows us to probe the 9.03 GHz distant $6p'[3/2]_1 - 8s'[3/2]_1$ Xe I transition in the OGC as opposed to the typical 18.1 GHz distant $6s'[1/2]_1 - 6p'[3/2]_2$ Xe I transition, reducing the frequency range of each scan (and thus the time required) by half.[22,23] A typical 30 GHz laser scan is accomplished in ~ 8 minutes with a lock-in time constant of 3 seconds.

Choppers (Ch1 = 1.9 kHz and Ch2 = 2.5 kHz) are used for homodyne detection of the OGC and fluorescence signals. The majority of the probe beam (~ 50 mW) is sent into the vacuum chamber, in the axial direction towards the thruster plume. The resulting fluorescence is collected at a 60° angle from the probe beam axis using a 200 mm focal length lens with 100 mm diameter. The collimated fluorescence signal is directed through a window in the chamber side wall to a similar lens that focuses the collected fluorescence onto the entrance slit of the 125 mm focal length monochromator attached to a photomultiplier tube (PMT). If sent directly into a lock-in amplifier, the resulting signal would be a time-averaged measurement of the fluorescence excitation lineshape. To synchronize the LIF signal in time to the discharge current, a sample-hold scheme is implemented between the PMT and the lock-in. The development of this sample-hold scheme is described elsewhere.[12,13,24]

The sample-hold method relies on an acquisition gate locked at a given phase of the discharge current oscillation period of the thruster. The acquisition gate is generated by a pulse-delay generator (Stanford Research Systems DG535) triggered by a voltage comparator chip (Model LM339). During the acquisition gate, the PMT signal (emission plus fluorescence) is sampled, averaged and held until the next trigger, at which point the held signal is updated (once per period). This method is well-suited for synchronizing with the naturally drifting current oscillations in the BHT-600 and we choose a gate width of 1 μs to be greater than the characteristic 0.7 μs fluctuations in oscillation period (obtained through the FWHM of the FFT in Fig. 2) to average out some of the jitter in the last few acquisition gates of the cycle. The sample-held signal is then sent through a lock-in amplifier for homodyne detection, constructing the IVDF from the fluorescence contribution originating only at a particular phase of the discharge oscillation.

Translating the acquisition gate in time along the current cycle allows the full time evolution of the fluorescence excitation lineshape (and thereby IVDF) to be reconstructed. To reduce data acquisition time, the sample-hold circuitry in this work is parallelized. The PMT signal is split into several sample-hold branches, each triggered at different phases in the discharge current cycle with a 1 μs gate width, as shown

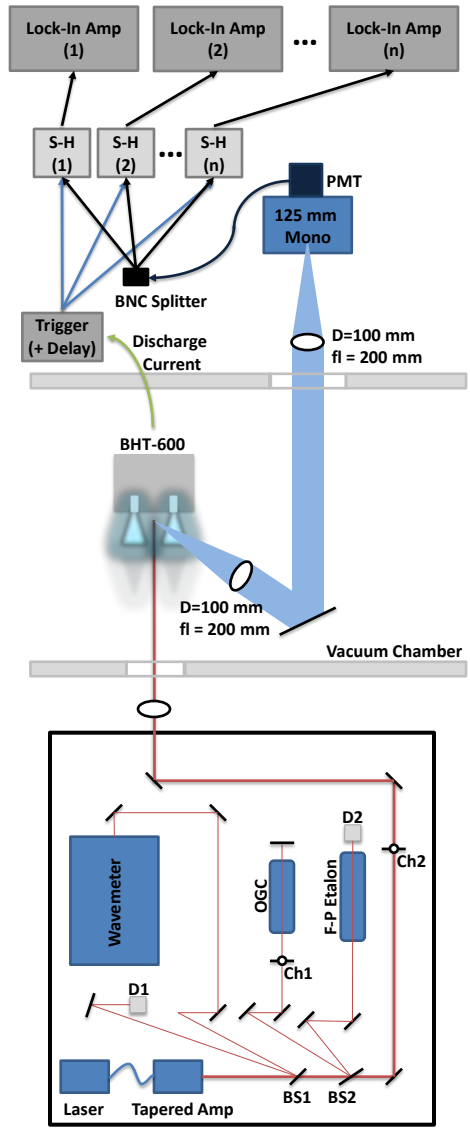

Figure 3: Laser optical train, including launch and collection optics, and parallelized sample-hold scheme.

in Fig. 3. This enables measurements of the IVDFs at six temporal points during a single laser scan, for a total of 23 points of time resolution (plus one time-averaged trace) in as few as 4 laser scans. We estimate that this parallelization, in conjunction with higher S/N due to increased laser power and printed sample-hold circuit design, plus the use of a new zero velocity reference transition, produces a factor of 9 improvement in the overall efficiency of data acquisition over previous work.

III. Results and Discussion

Time-synchronized axial ion velocity measurements are taken at numerous spatial points throughout the BHT-600 discharge channel and near-field plume. The results described here focus on the discharge channel, where the majority of ion acceleration takes place.

Figure 4 shows the variation in (a) most probable ion velocity and (b) peak lineshape intensity over the period of a typical discharge current oscillation along the thruster acceleration channel centerline ($R = 28$ mm). The boxes at right show equivalent results obtained from time-averaged LIF velocimetry. The most probable ion velocity is defined as the peak velocity of a Gaussian fit of the (primarily Doppler broadened)

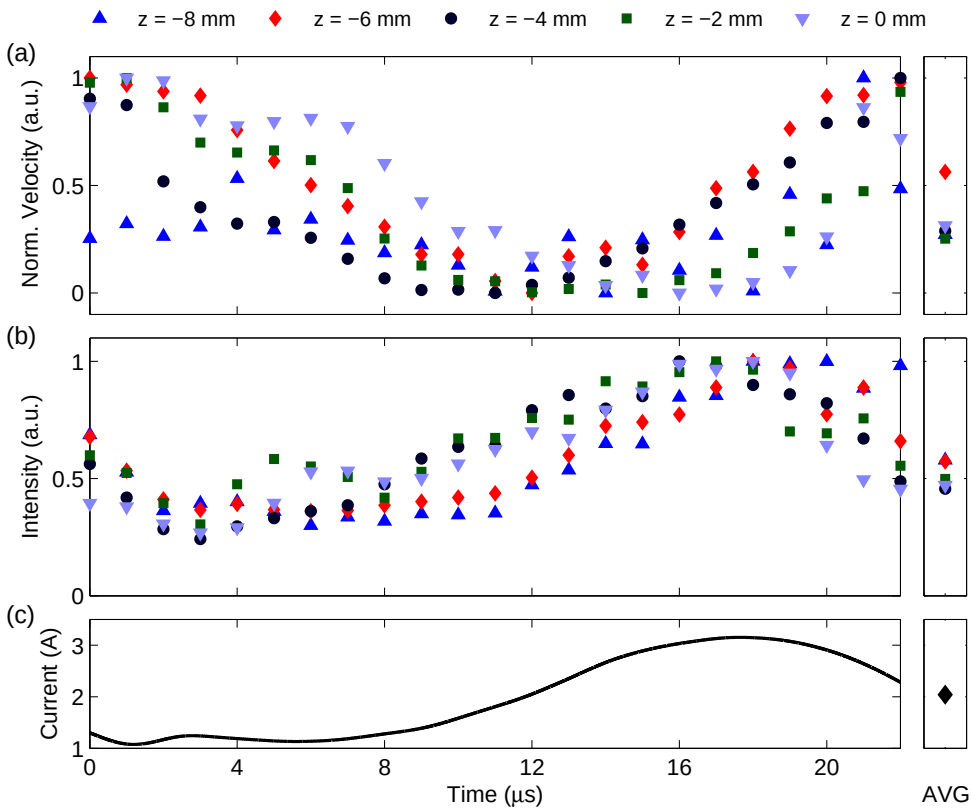

Figure 4: Trends along the acceleration channel centerline for (a) most probable axial ion velocities normalized by the total variation: $(V - V_{\min})/(V_{\max} - V_{\min})$, and (b) peak fluorescence excitation lineshape intensity over the (c) discharge current cycle. The boxes at right show the equivalent results from a time-averaged measurement.

fluorescence excitation lineshape and is shown here normalized by the total variation over the cycle: $(V - V_{\min})/(V_{\max} - V_{\min})$. Throughout the channel, the velocities follow the same overall pattern relative to the discharge current cycle, reaching their maxima about 1/4 oscillation period after the discharge current peak (90° phase lag). The velocities then fall to their minima as the discharge current begins its next ramp up.

The variations in the peak intensity of the measured fluorescence excitation lineshapes also follow the same overall trend throughout the current cycle, all throughout the acceleration channel. The intensity profiles closely track the current oscillation, and at some spatial locations the small inflections seen in the first 8 μs of the current trace can be observed in both the intensity and velocity plots. The relative fluorescence intensity at a given phase in the current cycle is related to the metastable Xe II probed state density ($5d[4]_{7/2}$). This population is assumed to follow that of the ground state ion density in the thruster plasma.

The observed trends may be interpreted according to standard models of the breathing mode.[9,10] The discharge current increases as an ionization front moves upstream, consuming neutral propellant and increasing the population of free electrons. The fluorescence intensity consequently increases as the ion population grows. The newly generated ions accelerate out of the channel according to the local potential field that is also changing with time. Ions obtain their maximum velocity soon after the point of peak ionization, and the ion density (and measured intensity) necessarily falls as the ions accelerate. The ionization front moves back downstream during the discharge current trough, the neutral population builds, and eventually the channel is left with slower ions that did not experience as large of a potential drop as the others. The cycle repeats as the discharge current ramps up again.

Figure 5 shows the evolution of the time-synchronized ion velocity distributions over the course of a typical discharge current cycle for spatial points spanning the entire channel. The anode is located at $Z = -10$ mm (bottom of the figure), the exit plane is at $Z = 0$ (top), the inner channel wall is at $R = 24$ mm (left),

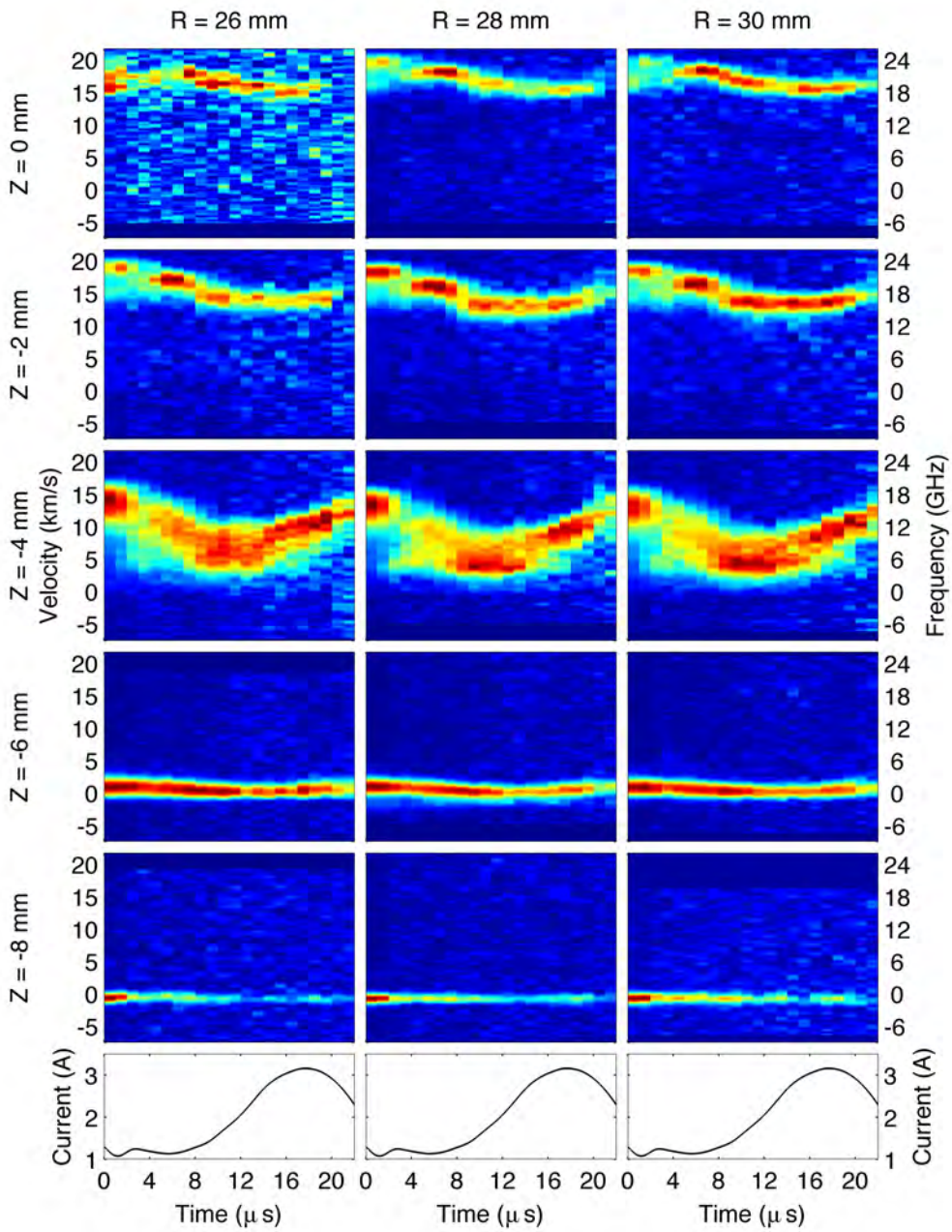

Figure 5: Time-varying axial ion velocity distributions for a typical breathing mode current cycle at several locations in the thruster channel. The anode is at $Z = -10$ mm and the exit plane is $Z = 0$ mm. The color scale spans blue (minimum) – red (maximum), with higher values indicating a narrower distribution.

and the outer channel wall is at $R = 32$ mm (right). Each of the individual IVDF traces obtained in a 1 μs acquisition gate constitutes one vertical band in each panel and is normalized by the total intensity of the fluorescence signal (sum of all values) collected from that scan. This choice of presentation indicates the temporal resolution of the data and the extent of the main fluorescence feature in velocity space (with higher values – more red – indicating a narrower distribution).

Figure 5 highlights the the spatial and temporal extent of ion acceleration in the BHT-600 channel. We observe only minimal radial variations in the time-synchronized velocity profiles. At $Z = -8$ mm near the anode, ions have a small negative velocity ~ -800 m/s over the whole cycle. This behavior can be attributed to a gradient-driven field reversal, often seen in hybrid Hall thruster simulations.[25,26] Moving downstream

to $Z = -6$ mm, the velocity distributions widen slightly, fluctuating in time between measured peaks of -200 and 800 m/s. Temporal variations in the IVDF (and thus accelerating potential) begin to emerge at this point.

The majority of channel acceleration occurs near $Z = -4$ mm, where the velocity distributions broaden significantly and show large temporal variations over the course of the current cycle. This indicates that both the spatial extent of propellant ionization and local potential significantly fluctuate in this region. Most probable ion velocities are observed between 5–13.2 km/s. These results especially illustrate the trends discussed above in conjunction with Fig. 4. As the discharge current ramps up between $\sim$8–14 μs, the ionization front (and presumably, the steeper part of the accelerating potential drop) is located downstream of $Z = -4$ mm since the measured velocities are at their lowest. Then, more ions are produced and accelerated as the ionization front and potential drop move upstream during the $\sim$ 14–20 μs interval of peak discharge current. As the current falls past 20 μs to $\sim$ 2 μs after the trigger, the strong potential drop is presumably upstream of $Z = -4$ mm, as the measured ion velocities remain roughly constant near their maximum values. Finally, the potential drop moves downstream again while the current is minimum. The relatively fewer remaining ions experience less and less of the accelerating potential drop, manifested in an observed decrease in ion velocity at $Z = -4$ mm.

Closer to the channel exit at $Z = -2$ mm and $Z = 0$, the IVDFs narrow again and the absolute velocity fluctuation is less pronounced, indicating that over time the majority of ions have been accelerated evenly. This indicates less spatial and temporal variation in ion production and accelerating potential compared with upstream. As shown in Fig. 6, the magnitude of velocity fluctuations over time and further ion acceleration continue to diminish as one moves farther downstream into the near-field plume.

A complementary view of the acceleration of ions in the channel is provided in Fig. 7, where the most probable ion velocities are plotted as a function of axial position down the channel centerline at a few instants in time. Again, the majority of ion acceleration is observed to occur between $Z = -6$ mm and $Z = -2$ mm, with a steeper velocity gradient that develops at early times in the cycle (low discharge current) giving way to more gradual ion acceleration during $t = 8 - 16$ μs. As the discharge current passes its maximum, the spatial acceleration profile becomes steeper again. Note that the more gradual time-averaged acceleration profile seems to be weighted towards the time interval during which the fluorescence intensity is stronger. Previous time-averaged LIF measurements of the BHT-600 confirm that the majority of ion acceleration is expected to occur inside the channel.[27]

IV. Future Work

In addition to the channel measurements presented here, time-synchronized axial IVDFs were obtained at various positions throughout the near-field plume. Figure 8 shows a representative IVDF time history for a point along the thruster axis at $Z = 15$ mm, $R = 0$ mm. At this position, two ion velocity populations are present throughout much of the breathing mode cycle. When the discharge current is minimum, the slower velocity population dominates at $\sim$ 5 km/s. As the discharge current increases, this population is assumed to wash out due to a wave of high axial velocity ions arriving from the channel.

There are several potential causes for secondary slow ion populations to appear throughout the near-field plume, including charge exchange collisions with neutrals, geometric effects from opposing sides of the channel, and residual ionization downstream of the main potential drop. Geometric effects in the BHT-600 were demonstrated previously in time-averaged LIF velocity measurements[27] and future analysis will seek to explain the emergence of multiple ion populations over time such as those observed in Fig. 8. Upcoming time-synchronized radial velocity measurements will yield the time histories of the magnitude and direction of the total ion velocity vectors, and may correlate fluctuations in the plume divergence angle with the discharge current cycle. These and other results will also be compared with numerical models of the BHT-600 from HPHall, which have previously obtained good agreement with time-averaged properties but failed to fully capture transient fluctuations observed in optical emission data.[16]

V. Conclusions

This work presents time-synchronized CW-LIF velocity measurements of a BHT-600 Hall thruster. The sample-hold time synchronization method correlates axial velocity distribution functions with the 48 kHz breathing mode discharge current cycle of the thruster. Upgrades to the time-synchronized LIF apparatus

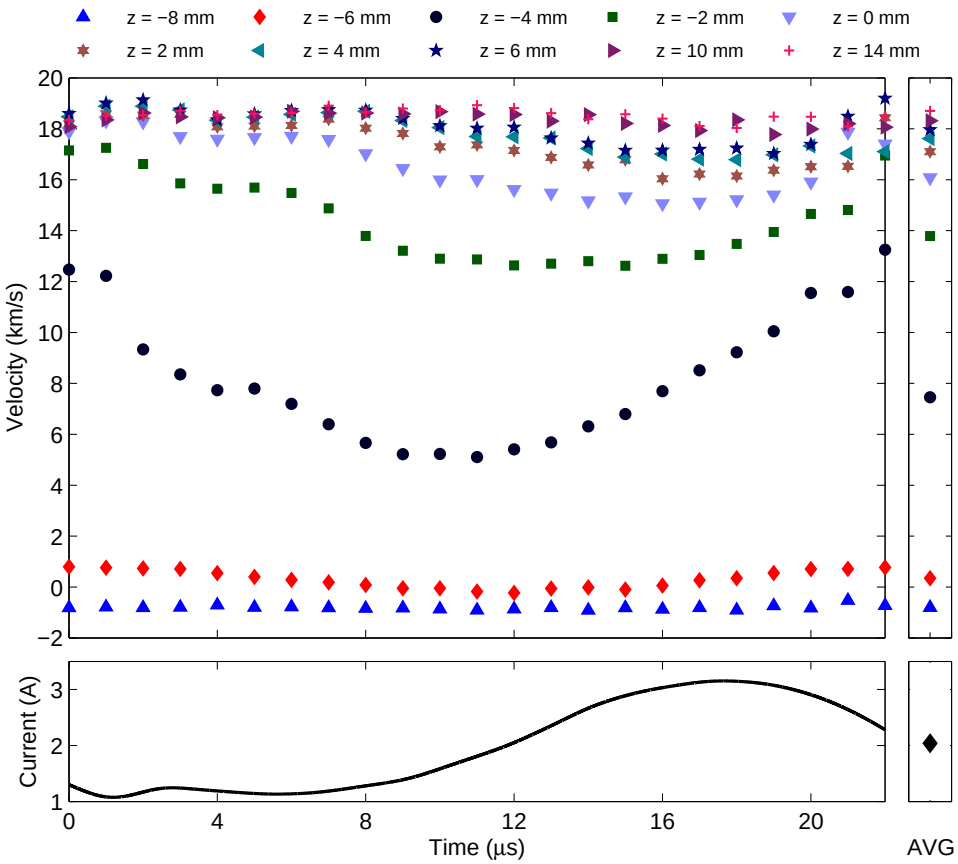

Figure 6: Most probable axial ion velocities along the centerline of the discharge channel and into the near-field plume.

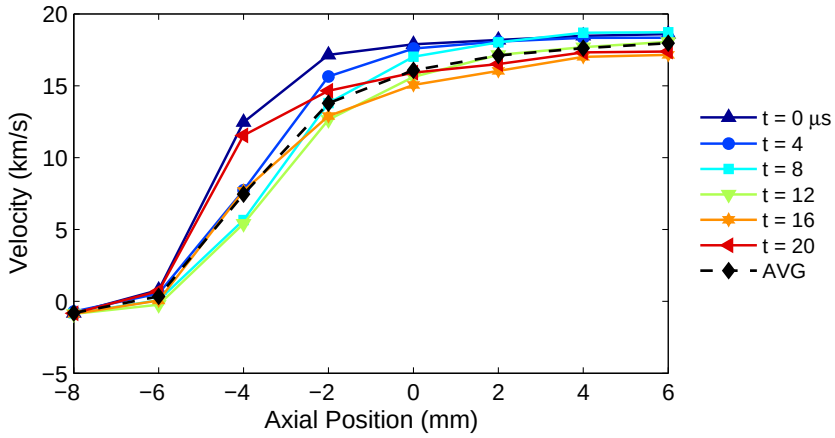

Figure 7: Most probable axial ion velocities along the channel centerline plotted as a function of space at 4 μs intervals.

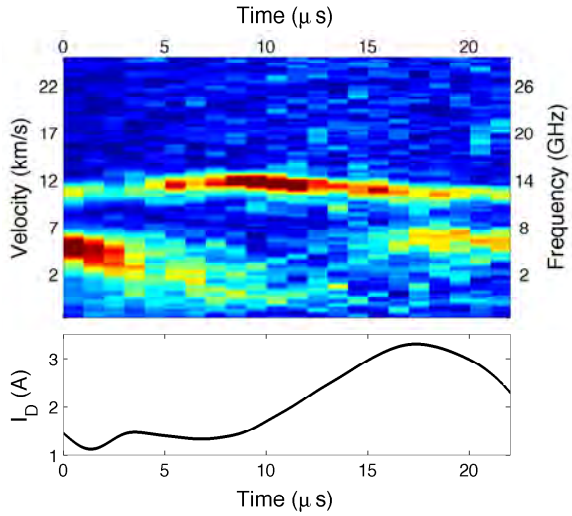

Figure 8: Axial ion velocity distributions vs. time at $Z = 15$ mm, $R = 0$ mm.

used previously increased measurement signal-to-noise and allowed for significantly faster data acquisition. This enabled a much more extensive spatial mapping of the thruster plume than in previous work.

Axial ion velocity distributions over the entire discharge current cycle are presented at spatial points throughout the thruster acceleration channel with a time resolution of 1 μs. The measured fluorescence excitation lineshape intensities rise and fall in phase with the discharge current, indicating temporal changes in ion density. The most probable velocities follow a similar trend, lagging the current in phase by approximately 1/4 of the oscillation period. The observed patterns are consistent with models of the breathing mode and previous time-resolved LIF measurements on a different laboratory Hall thruster. The majority of axial ion acceleration is seen between $Z = -6$ mm and $Z = -2$ mm, where the broadest IVDFs also vary the most in magnitude over time. As the ions accelerate into the near-field plume, the axial ion velocities plateau and fluctuations across the breathing mode period diminish. Future work will discuss the time variation of the rest of the plume, present measurements of the radial ion velocity components, and make comparisons with BHT-600 Hall thruster simulations.

Acknowledgments

This work is sponsored in part by the U.S. Air Force Office of Scientific Research with Dr. M. Birkan as program manager. C.Y. acknowledges support from the DOE NSSA Stewardship Science Graduate Fellowship under contract DE-FC52-08NA28752 and the Stanford Graduate Fellowship.

References

[1]Skiff, F. and Bollinger, J., "Mini-conference on laser-induced fluorescence in plasmas," *Physics of Plasmas*, Vol. 11, No. 5, 2004, pp. 2972–2975.

[2]Manzella, D. H., "Stationary Plasma Thruster Ion Velocity Distribution," *Proceedings of the 30th AIAA/ASME/SAE/ASEE Joint Propulsion Conference & Exhibit*, No. AIAA-1994-3141, Indianapolis, IN, June 27-29 1994.

[3]Hargus Jr., W. A. and Cappelli, M. A., "Laser-induced fluorescence measurements of velocity within a Hall discharge," *Applied Physics B*, Vol. 72, No. 8, 2001, pp. 961–969.

[4]Pelissier, B. and Sadeghi, N., "Time-resolved pulse-counting lock-in detection of laser induced fluorescence in the presence of a strong background emission," *Review of Scientific Instruments*, Vol. 67, 1996, pp. 3405–3410.

[5]Mazouffre, S. and Bourgeois, G., "Spatio-temporal characteristics of ion velocity in a Hall thruster discharge," *Plasma Sources Science and Technology*, Vol. 19, 2010, pp. 065018.

[6]Dannenmayer, K., Kudrna, P., Tichy, M., and Mazouffre, S., "Time-resolved measurement of plasma parameters in the far-field plume of a low-power Hall effect thruster," *Plasma Sources Science and Technology*, Vol. 21, 2012, pp. 055020.

[7]Durot, C. J., Gallimore, A. D., and Smith, T. B., "Validation and evaluation of a novel time-resolved laser-induced fluorescence technique," *Review of Scientific Instruments*, Vol. 85, No. 013508, 2014, pp. 1–14.

[8]Diallo, A., Keller, S., Shi, Y., Raitses, Y., and Mazouffre, S., "Time-resolved ion velocity distribution in a cylindrical Hall thruster: Heterodyne-based experiment and modeling," *Review of Scientific Instruments*, Vol. 86, No. 3, 2015, pp. 033506.

[9]Boeuf, J.-P. and Garrigues, L., "Low frequency oscillations in a stationary plasma thruster," *Journal of Applied Physics*, Vol. 84, No. 7, 1998, pp. 3541.

[10]Barral, S. and Ahedo, E., "Low-frequency model of breathing oscillations in Hall discharges," *Physical Review E*, Vol. 79, No. 4, 2009, pp. 046401.

[11]Fife, J., Martinez-Sanchez, M., and Szabo, J., "A numerical study of low-frequency discharge oscillations in Hall thrusters," *Proceedings of the 33rd AIAA/ASME/SAE/ASEE Joint Propulsion Conference & Exhibit*, No. AIAA-1997-3052, Seattle, WA, 6-9 July 1997.

[12]MacDonald, N. A., Cappelli, M. A., and Hargus Jr., W. A., "Time-synchronized continuous wave laser-induced fluorescence axial velocity measurements in a diverging cusped field thruster," *Journal of Physics D: Applied Physics*, Vol. 47, No. 11, 2014, pp. 115204.

[13]Young, C. V., Lucca Fabris, A., and Cappelli, M. A., "Ion dynamics in an $E \times B$ Hall plasma accelerator," *Applied Physics Letters*, Vol. 106, No. 4, February 2015, pp. 044102.

[14]Ekholm, J. M., Hargus, Jr., W. A., Larson, C. W., Nakles, M. R., Reed, G. D., and Niemela, C. S., "Plume Characteristics of the Busek 600 W Hall Thruster," *Proceedings of the 42nd AIAA/ASME/SAE/ASEE Joint Propulsion Conference & Exhibit*, No. AIAA-2006-4659, July 2006.

[15]Victor, A., Zurbuchen, T., and Gallimore, A., "Ion-Energy Plume Diagnostics on the BHT-600 Hall Thruster Cluster," *Journal of Propulsion and Power*, Vol. 22, No. 6, 2008, pp. 1421–1424.

[16]Gonzales, A. E., Koo, J. W., and Hargus Jr., W. A., "Comparison of Numerical and Experimental Time-Resolved Near-Field Hall Thruster Plasma Properties," *IEEE Transactions on Plasma Science*, Vol. 42, No. 3, 2014, pp. 806–812.

[17]Hargus, Jr., W. A. and Charles, C. S., "Near Exit Plane Velocity Field of a 200-Watt Hall Thruster," *Journal of Propulsion and Power*, Vol. 24, No. 1, 2008, pp. 127–133.

[18]Hansen, J. E. and Persson, W., "Revised Analysis of Singly Ionized Xenon, Xe II," *Physica Scripta*, Vol. 36, No. 4, 1987, pp. 602–643.

[19]MacDonald, N. A., Young, C. V., Cappelli, M. A., and Hargus Jr., W. A., "Ion velocity and plasma potential measurements of a cylindrical cusped field thruster," *Journal of Applied Physics*, Vol. 111, No. 9, 2012, pp. 093303.

[20]Mazouffre, S., Gawron, D., Kulaev, V., and Sadehgi, N., "Xe+ Ion Transport in the Crossed-Field Discharge of a 5-kW-Class Hall Effect Thruster," *IEEE Transactions on Plasma Science*, Vol. 36, No. 5, October 2008, pp. 1967–1976.

[21]MacDonald, N. A., Loebner, K., and Cappelli, M. A., "Time Synchronized Optical Diagnostics of a Diverging Cusped Field Ion Accelerator," *Bulletin of the 64th Annual Gaseous Electronics Conference*, Vol. 56, Salt Lake City, UT, November 14-18 2011.

[22]Miller, M. H. and Roig, R. A., "Transition Probabilities of Xe I and Xe II," *Physical Review A*, Vol. 8, No. 1, July 1973, pp. 480–486.

[23]Kramida, A., Ralchenko, Y., Reader, J., and and NIST ASD Team, NIST Atomic Spectra Database (ver. 5.2), [Online]. Available: `http://physics.nist.gov/asd` [2015, May 15]. National Institute of Standards and Technology, Gaithersburg, MD., 2014.

[24]MacDonald, N. A., Cappelli, M. A., and Hargus Jr., W. A., "Time-Synchronized CW Laser-Induced Fluorescence on an Oscillatory Xenon Discharge," *Review of Scientific Instruments*, Vol. 83, 2012, pp. 113506.

[25]Scharfe, M. K., Gascon, N., Cappelli, M. A., and Fernandez, E., "Comparison of hybrid Hall thruster model to experimental measurements," *Physics of Plasmas (1994-present)*, Vol. 13, No. 8, 2006, pp. 083505.

[26]Parra, F., Ahedo, E., Fife, J., and Martinez-Sanchez, M., "A two-dimensional hybrid model of the Hall thruster discharge," *Journal of Applied Physics*, Vol. 100, No. 2, 2006, pp. 023304.

[27]Hargus Jr., W. A. and Charles, C. S., "Near-Plume Laser-Induced Fluorescence Velocity Measurements of a Medium Power Hall Thruster," *Journal of Propulsion and Power*, Vol. 26, No. 1, 2010, pp. 135–141.

Time-Synchronized Continuous Wave Laser Induced Fluorescence Velocity Measurements of a 600 Watt Hall Thruster

34th International Electric Propulsion Conference

IEPC-2015-350/ISTS-2015-b-350

Tuesday, November 4, 2014

Integrity ★ Service ★ Excellence

Natalia MacDonald-Tenenbaum

(Air Force Research Laboratory)

Christopher Young & Andrea Lucca Fabris

(Stanford Plasma Physics Laboratory)

Michael Nakles

(ERC, Inc.)

William Hargus, Jr.

(Air Force Research Laboratory)

Mark Cappelli

(Stanford Plasma Physics Laboratory)

Outline

- Motivation
- BHT-600 Hall Thruster
  - Specifications
  - Operating Conditions
- Time-synchronized Laser Induced Fluorescence
  - Method, parallelization of measurements
  - Results
- Continuing Work
- Summary and Conclusions

Motivation

- **Laser induced fluorescence (LIF) velocimetry**
  - **Non-intrusive method of probing plasma**
  - **High spatial resolution**
  - **Sample-hold method used to provide time resolution for naturally occurring quasi-periodic discharges**
- **Time-resolved ion velocity distribution functions (IVDFs):**
  - **Provide insight into dynamics of thruster operation**
  - **Are linked to thruster performance metrics**
  - **Are critical to validating numerical simulations**

- **Motivation for this work:**
  - **Demonstrate efficient data collection for parallelized method of time-sync LIF**
  - **Apply method to well-documented Hall thruster for future comparisons to optical emission, probe data, numerical simulations, etc…**

BHT-600 Specifications

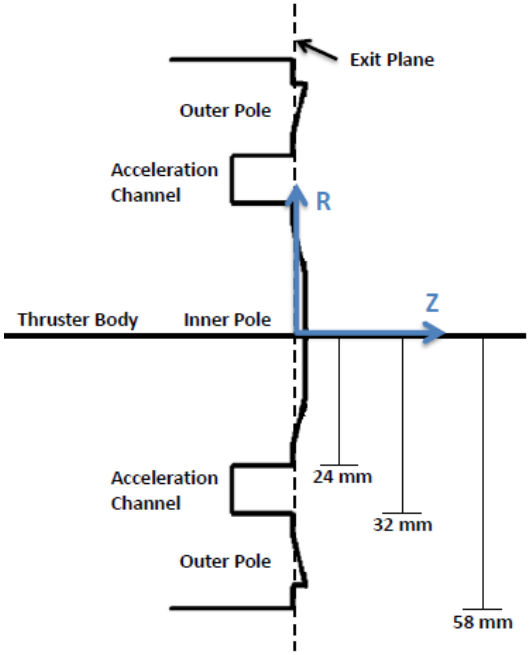

a) Schematic of BHT-600

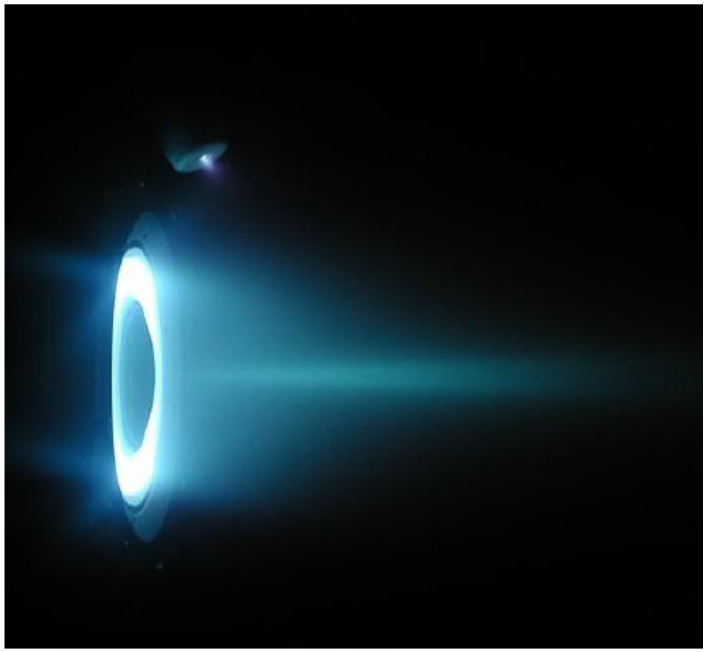

b) BHT-600 Operating on Xenon

Nominal Operating Conditions

Anode Flow	2.45 mg/s Xe (20.5 sccm)
Cathode Flow	197 μg/s Xe (1.5 sccm)
Anode Potential	300 V
Anode Current	2.05 A
Magnet 1 Current	2.0 A
Magnet 2 Current	2.0 A

- **600 W annular Hall thruster**
- **Manufactured by Busek Co.**
- **Tested in Chamber 6 at AFRL**

BHT-600 Operating Conditions

- **Quasi-periodic operation**
  - **f = 48 kHz**
  - **T = 21 μs**
- **1 μs gate width for triggering**
  - **21 points of time resolution**
  - **Allows for slight fluctuations in discharge period**

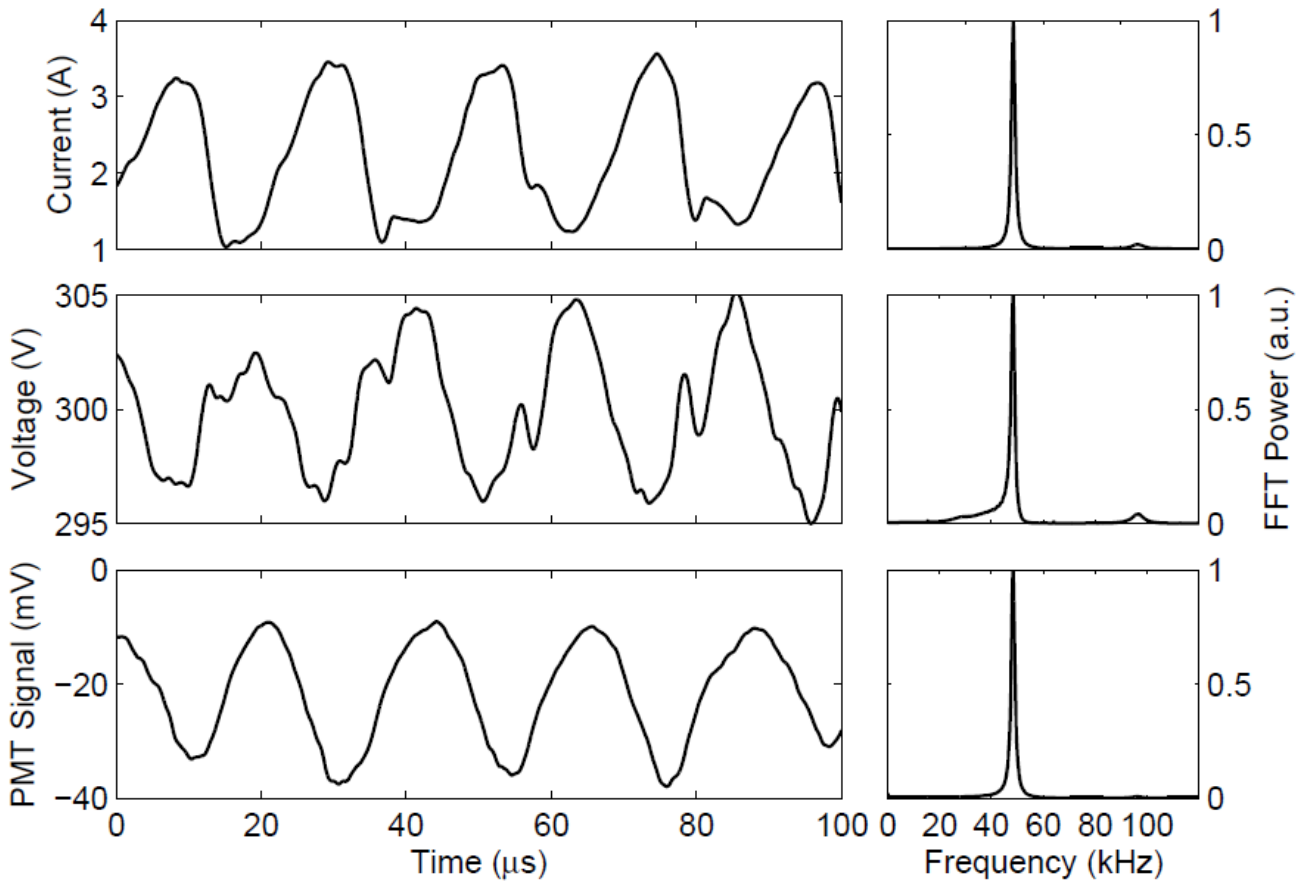

Experimental Apparatus

- **New Focus Vortex TLB-6917 tunable diode laser used to seed a TA-7600 VAMP tapered amplifier**
  - **60 mW output power**
  - **Xenon ion (Xe II) transition at 834.72 nm probed ($5d[4]_{7/2}$–$6p[3]_{5/2}$)**
  - **Non-resonant fluorescence collected at 541.92 nm ($6s[2]_{3/2}$ –$6p[3]_{5/2}$)**

- **Stationary xenon neutral (Xe I) reference**
  - **9.03 GHz distant $6p'[3/2]_1$–$8s'[3/2]_1$**

- **Parallelized sample-hold method of time-synchronization**
  - **6 time points taken simultaneously**

➢ **9x improvement in data acquisition efficiency**
  - ➢ **Better signal-to-noise**
  - ➢ **Faster data acquisition**

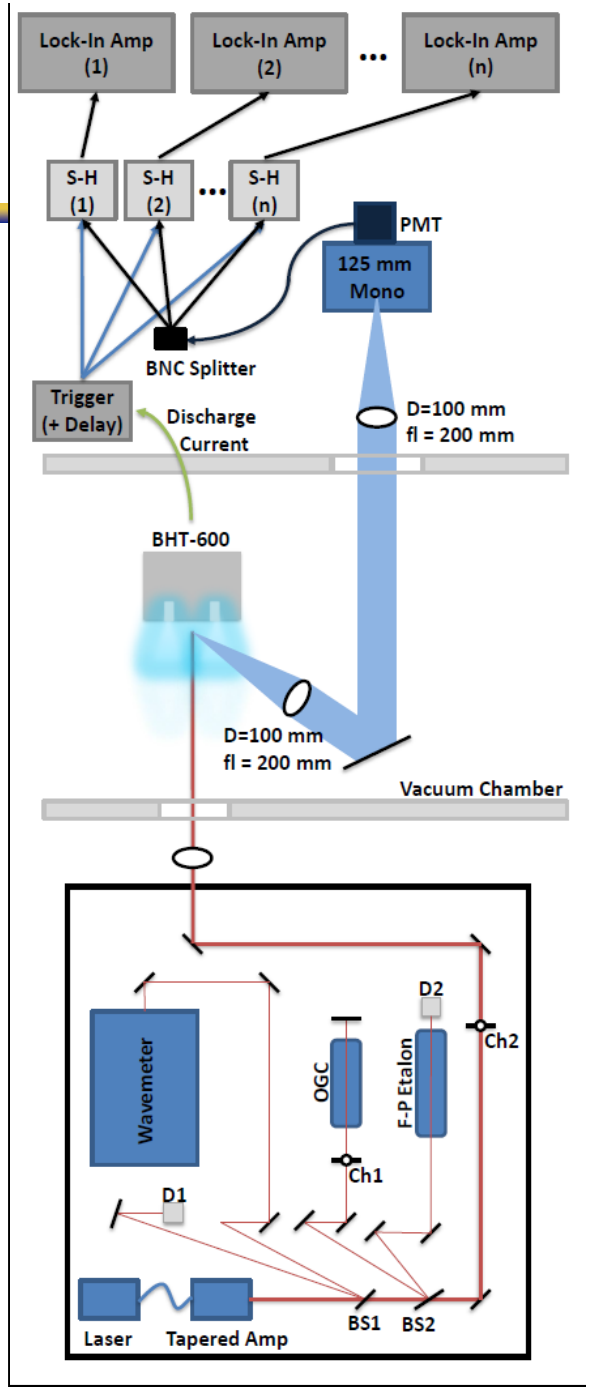

Velocity and Intensity Trends

- **Peak lineshape intensity**
  - **In phase with current**
  - **Intensity increases w/ growth of ion population**
- **Most probable ion velocity**
  - **90º phase lag relative to current**
  - **Max velocity after point of peak ionization**

➢ **Breathing mode cycle**

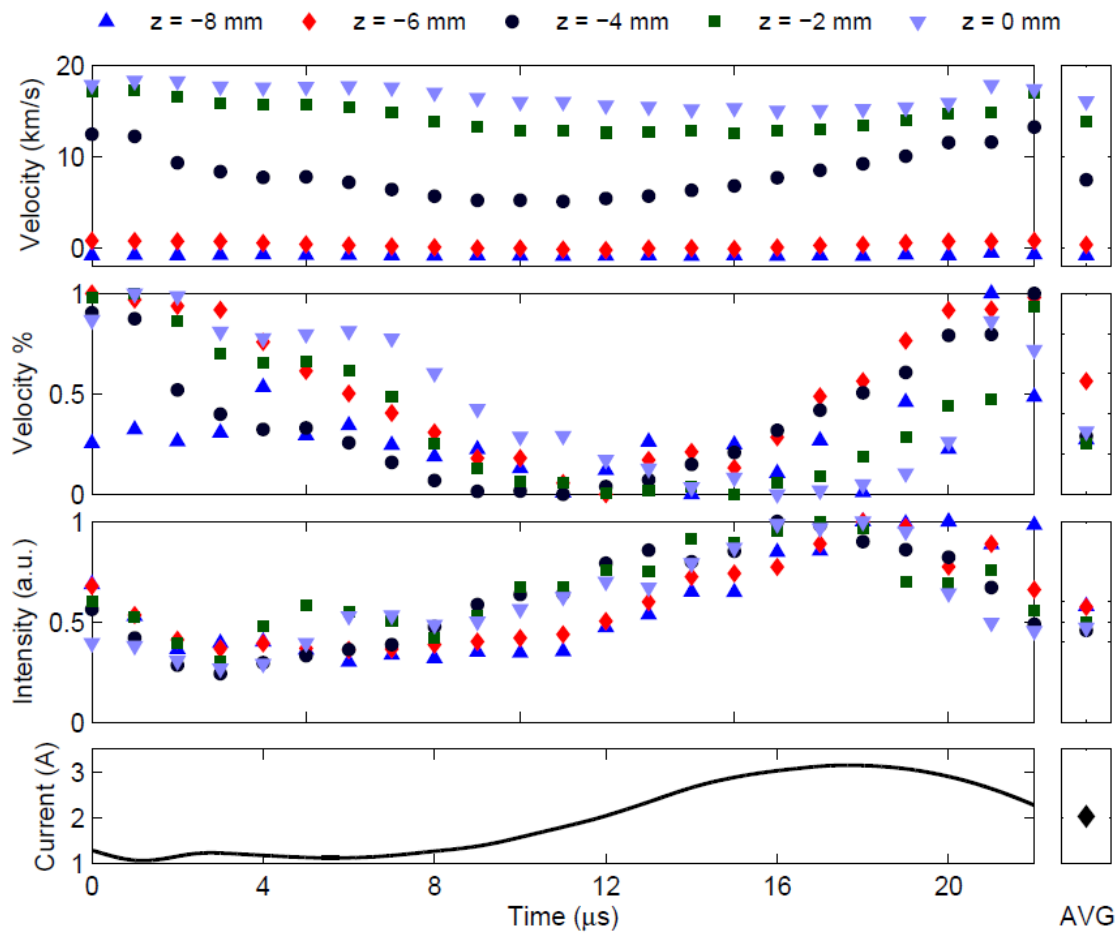

Most probable ion velocity and peak lineshape intensities for IVDFs measured along centerline of discharge channel (R = 28 mm)

Channel IVDFs

- **Minimal radial variations in channel**
- **Z = -8 mm (near anode)**
  - **Slight negative velocity**
  - **Gradient-driven field reversal**
- **Z = -6 mm**
  - **Accelerating potential begins**
  - **Broader IVDFs**
- **Z = -4 mm**
  - **Significant broadening of IVDFs**
  - **Large temporal variations (5-13 km/s)**
  - **Spatial extent of propellant ionization and local potential drop fluctuate**
- **Z = -2 mm, Z = 0 mm**
  - **IVDFs narrow**
  - **More even acceleration in time**

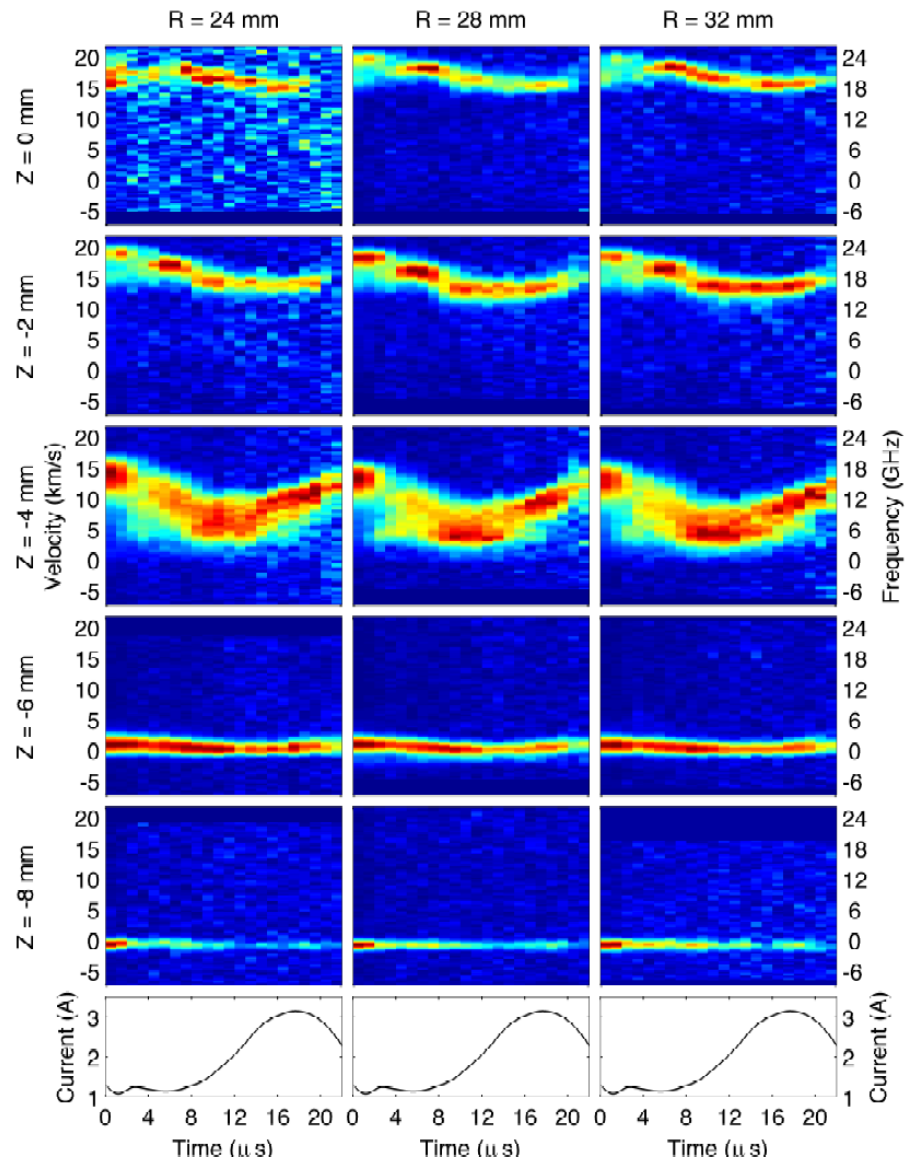

Channel Midline Velocities

- **Majority of ion acceleration between Z = -6 and -2 mm**
- **Steepest velocity gradients at minimum in discharge current**
- **Velocities relatively constant in near-field plume (past exit plane)**

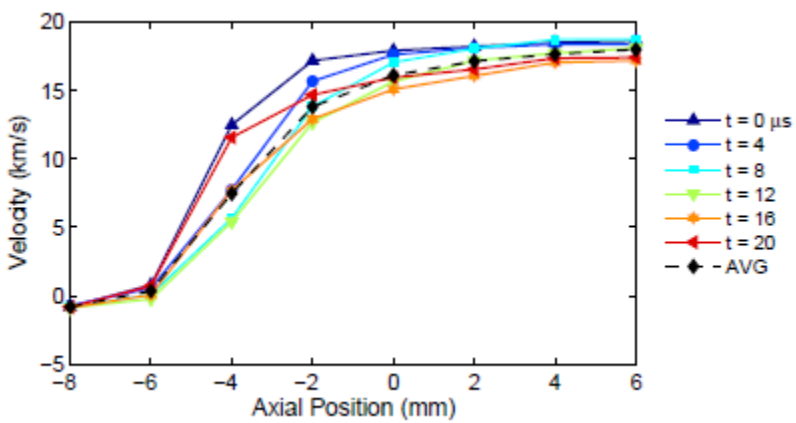

Most probable ion velocity as function of position along centerline

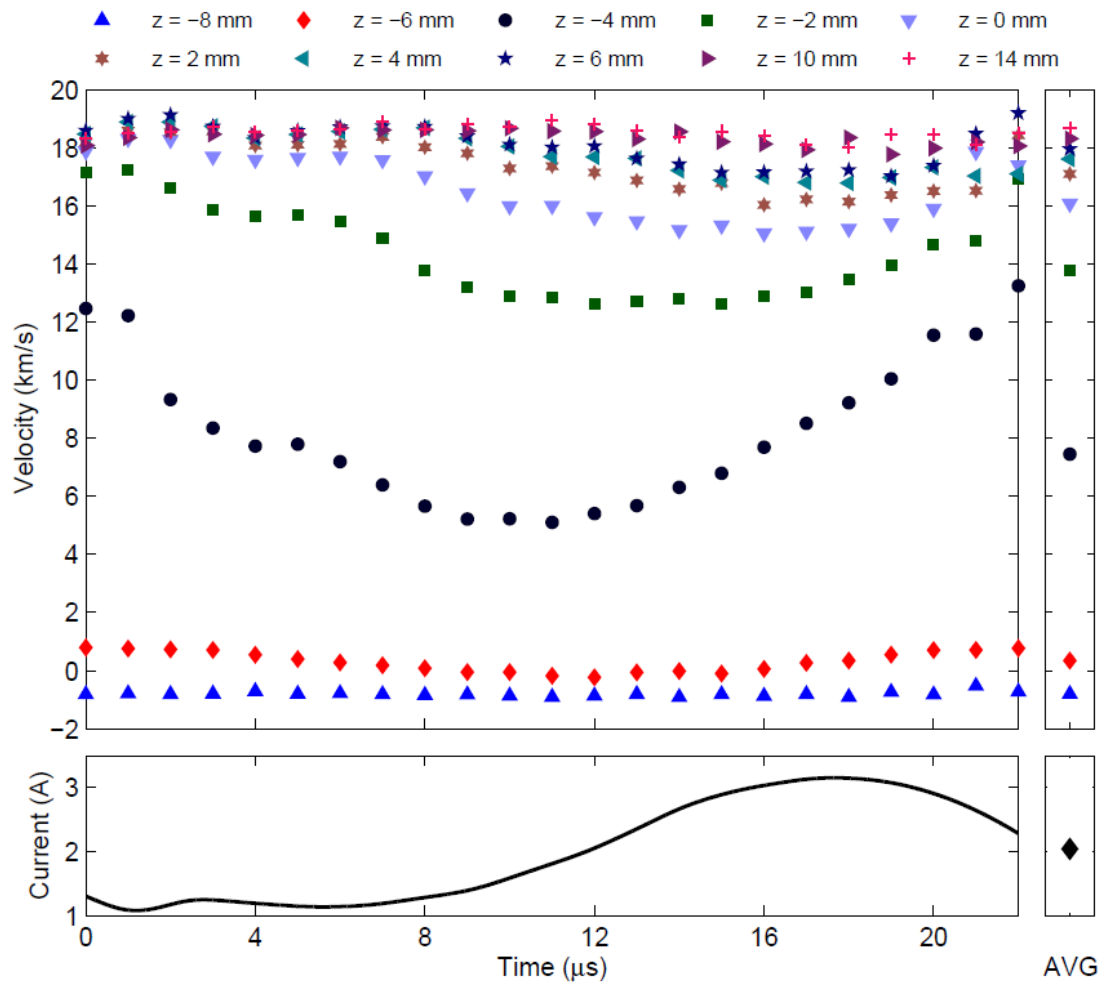

Most probable ion velocity extending into near-field plume along centerline of discharge channel (R = 28 mm)

Continuing Work

- **Time-sync axial IVDFs obtained throughout near-field plume**
- **Secondary ion velocity population**
  - **Appears near centerline of thruster**
  - **Low velocity dominates at current minimum**
  - **Primarily caused by geometric effects**
  - **Other causes:**
    - **Charge exchange collisions w/ neutrals**
    - **Residual ionization downstream of main potential drop**
- **Upcoming radial IVDF measurements**
  - **Elucidate fluctuations in plume divergence**
  - **Ion velocity vectors compared to numerical models in HPHall, emission data**

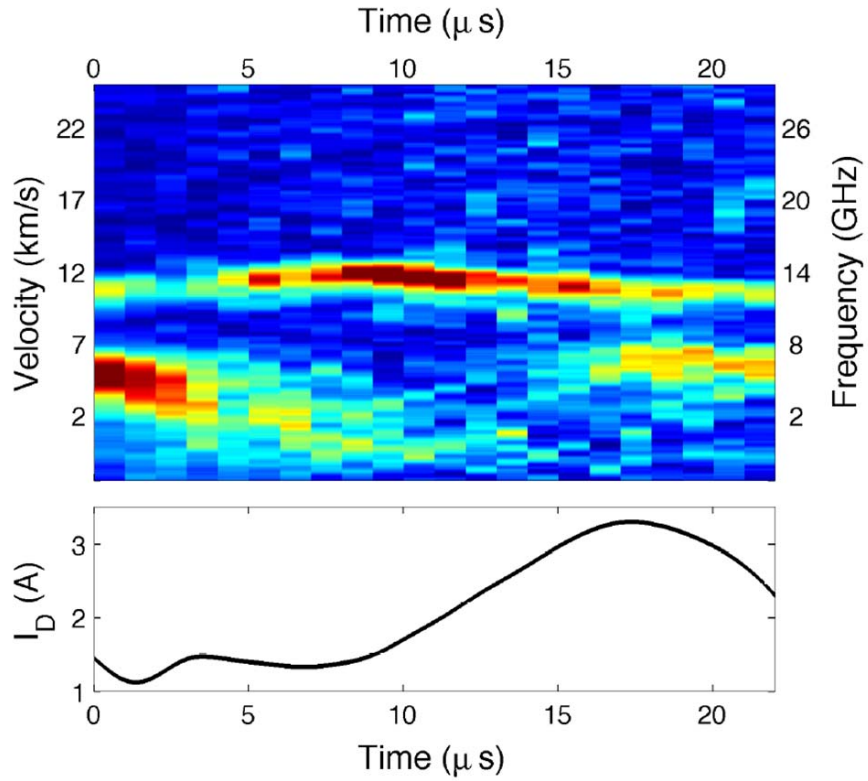

Axial ion velocity distributions vs. time at Z = 15 mm, R = 0 mm.

Summary

- **Axial ion velocity distribution functions correlated in time to 48 kHz breathing mode**
  - **Linshape intensities change in phase with discharge current**
  - **Most probable velocities 90º lag from discharge current**
  - **Consistent with breathing mode**

- **Upgraded time-synchronized LIF apparatus allowed for 9x more efficient data collection**
  - **Extensive spatial mapping of BHT-600 plume (60+ spatial points!!!)**
  - **Near-field plume measurements to be shown in future presentations**